STRUCTURAL SCIENCE
CRYSTAL ENGINEERING
MATERIALS

Volume 75 (2019)

Supporting information for article:

Octahedral tilting in the polar hexagonal tungsten bronzes RbNbW2O9 and KNbW2O9

Jason A. McNulty, Alexandra S. Gibbs, Philip Lightfoot and Finlay D. Morrison

Table S1 Comparison of the respective Rietveld refinements of PND data at 293 K for $KNbW_2O_9$ refined in various orthorhombic space groups featuring different unit cell dimensions.

Model	Metrics	χ^2	w*Rp* (%)	*Rp* (%)	N_{tot}
*Cmm*2	$3a_0 \times \sqrt{3}a_0 \times c_0$	112.6	19.81	15.03	72
$Cmc2_1$	$3a_0 \times \sqrt{3}a_0 \times 2c_0$	19.83	9.67	8.54	121
$Cmc2_1$	$\sqrt{3}a_0 \times 3a_0 \times 2c_0$	26.31	11.13	9.32	124
$Cmc2_1$	$\sqrt{3}a_0 \times a_0 \times 2c_0$	23.66	8.50	7.00	67
$Cmc2_1$	$a_0 \times \sqrt{3}a_0 \times 2c_0$	6.649	4.51	3.72	63

Table S2 Crystallographic data for $KNbW_2O_9$ at 293 K refined in the $Cmc2_1$ space group [a = 7.3195 (1), b = 12.6147 (3), c = 7.7511 (1) Å].

Atom	Wyckoff Position	*x*	*y*	*Z*	$100*U_{iso}$ (Å^2)
K1	4a	0	0.0020 (6)	0.1982 (11)	5.88 (16)
O1	4a	0	0.4718 (2)	0.2296 (11)	1.90 (8)
O2	8b	0.2797 (3)	0.2766 (1)	0.2378 (12)	1.71 (5)
O3	4a	0	0.2151 (6)	0.0240 (11)	1.08 (14)
O4	8b	0.6844 (7)	0.1042 (4)	0.0272 (4)	1.29 (11)
O5	4a	0	0.2118 (6)	0.4451 (12)	1.24 (16)
O6	8b	0.6866 (7)	0.1038 (4)	0.4574 (12)	1.07 (10)
Nb/W1	4a	0	0.4992 (3)	0.0275 (9)	1.15 (9)
Nb/W2	8b	0.2543 (12)	0.2543 (5)	0.0003 (10)	2.15 (6)

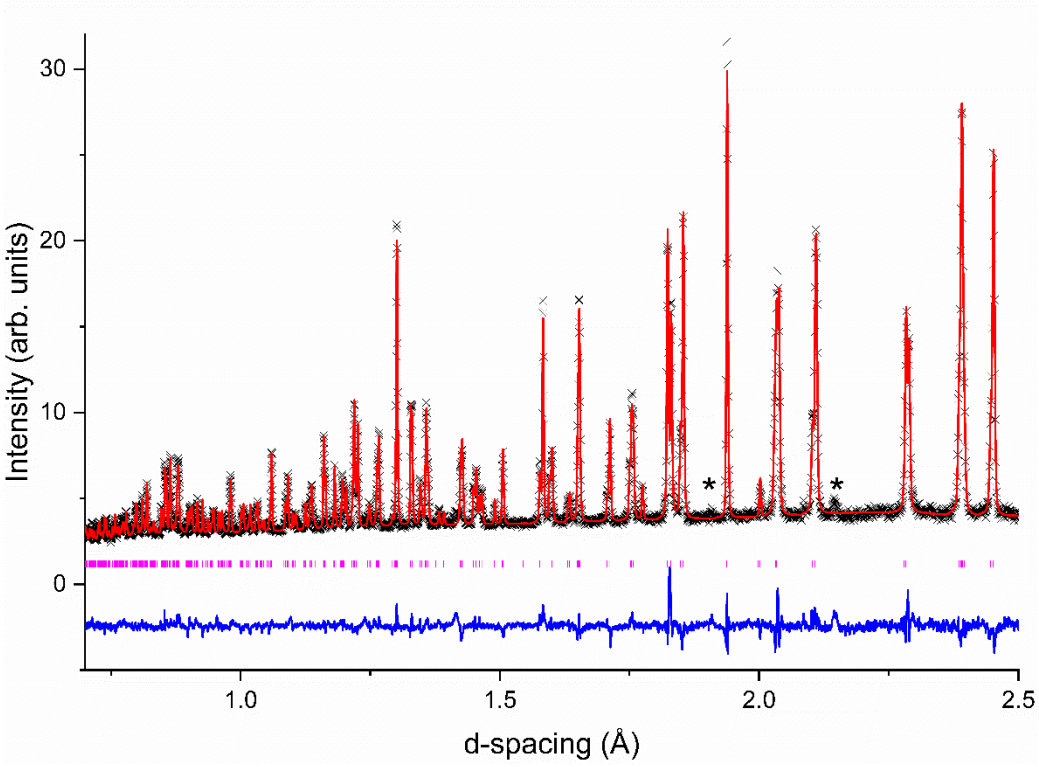

Figure S1 Portion of Rietveld refinement profile of $KNbW_2O_9$ PND data at 293 K using the simplest $Cmc2_1$ model (cell metrics $a_0 \times \sqrt{3}a_0 \times 2c_0$). The peaks marked '*' indicate peaks attributable to the vanadium can.

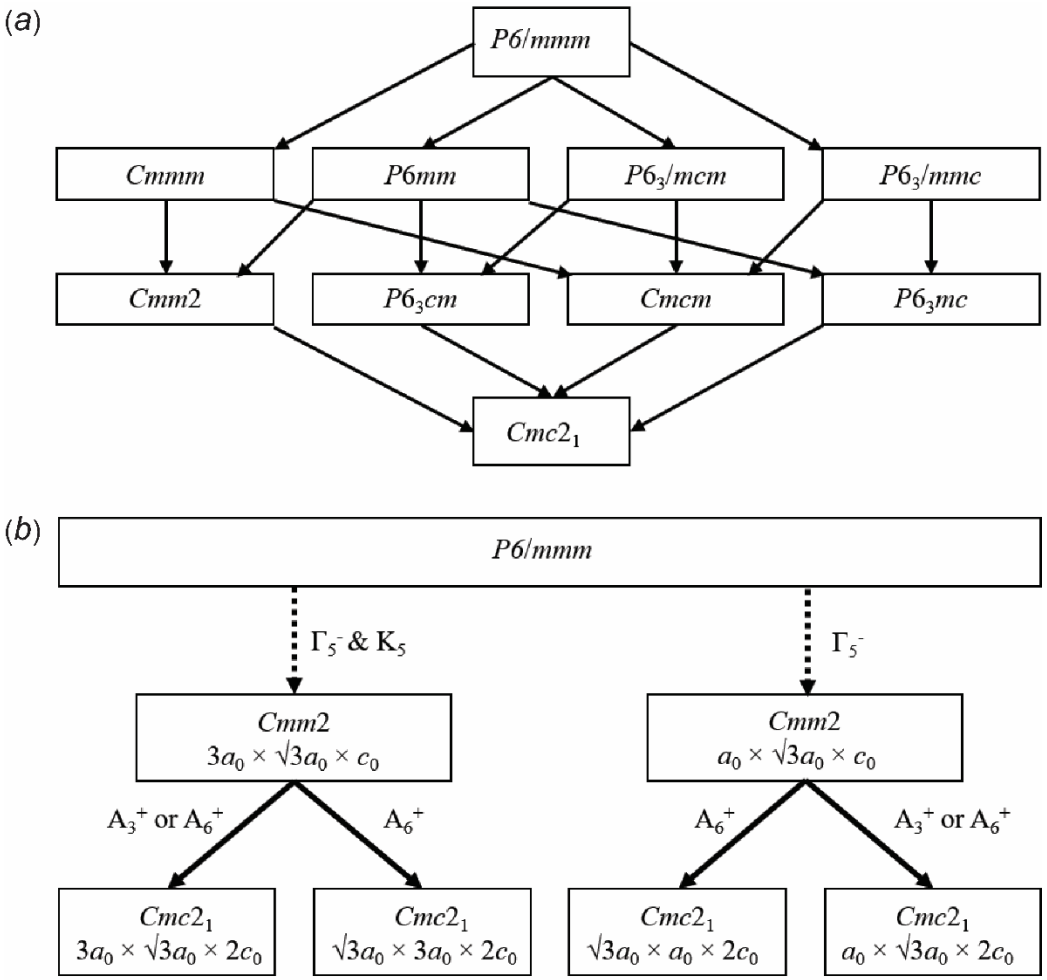

Figure S2 (a) Group-subgroup relations for $RbNbW_2O_9$ and $KNbW_2O_9$ derived from the *h*-WO_3/$Cs_{0.33}WO_3$ (*P*6/*mmm*) aristotype. Groups not connected to sub-groups by an arrow indicate that such a transition is required to be first order according to Landau theory. (b) Group-subgroup relation diagram indicating the distortion modes responsible for transformation from the parent *P*6/*mmm* to each of the *Cmc*2$_1$ models with different unit cell metrics. The larger *Cmm*2 model represents the structure published by Chang *et al.* (2008).

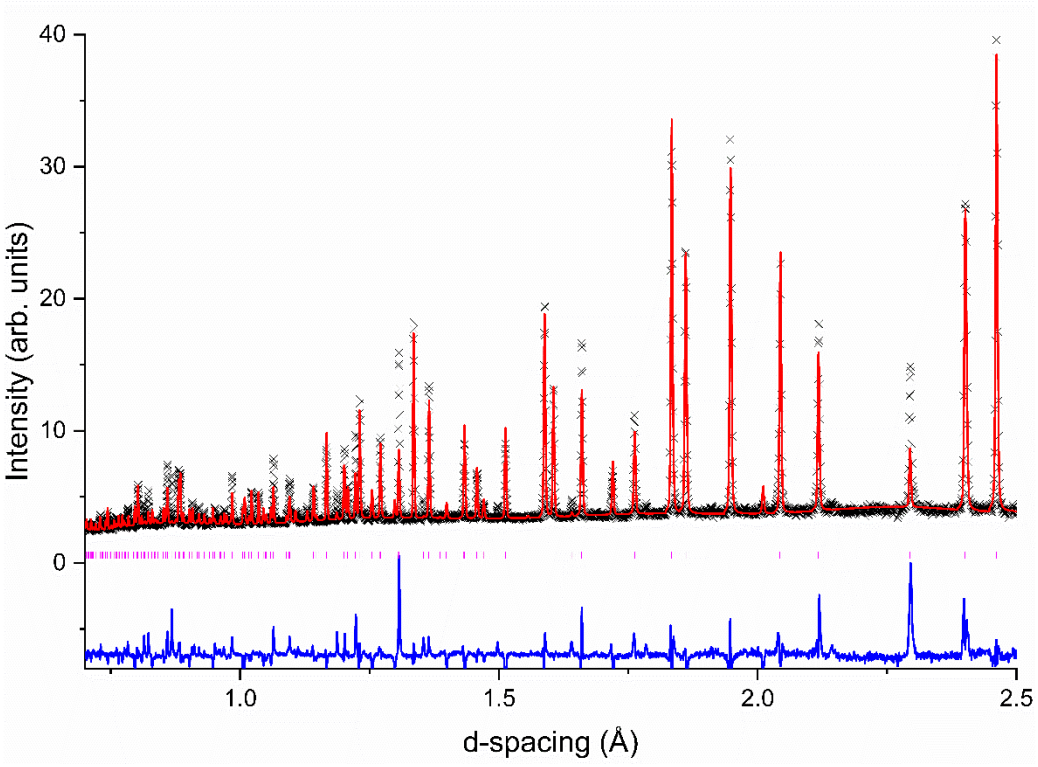

Figure S3 Portion of Rietveld refinement profile of $RbNbW_2O_9$ PND data at 288 K using the hexagonal $P6_3cm$ space group.

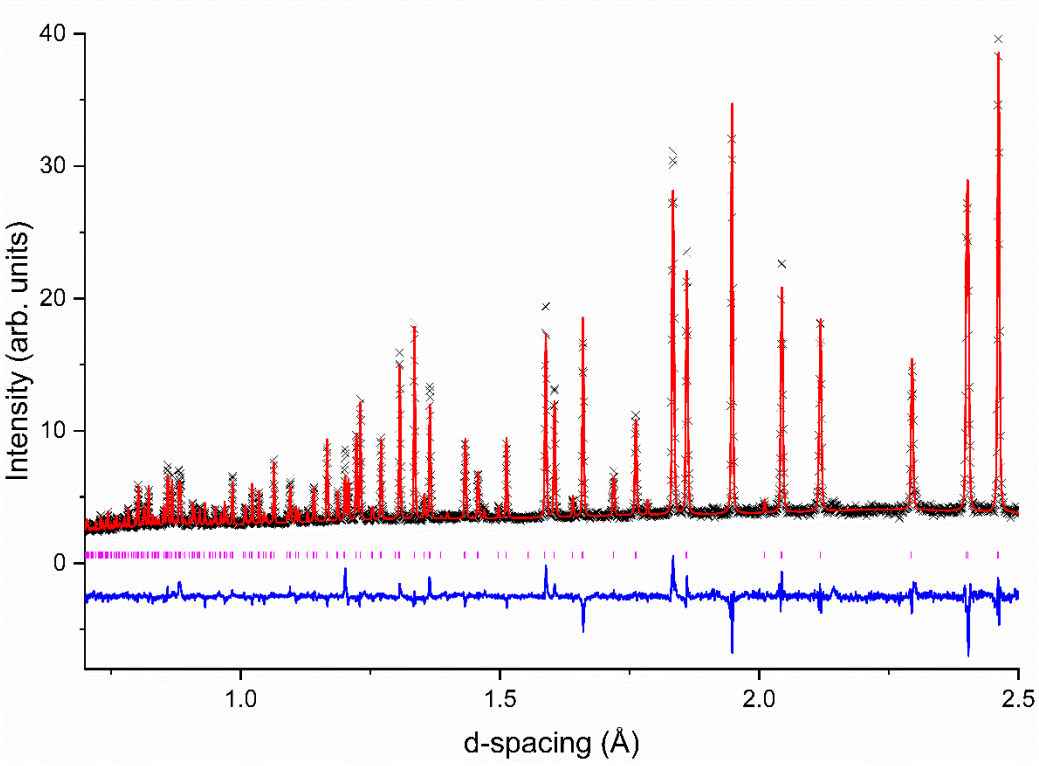

Figure S4 Portion of Rietveld refinement profile of $RbNbW_2O_9$ PND data at 288 K using the orthorhombic centrosymmetric *Cmcm* space group.

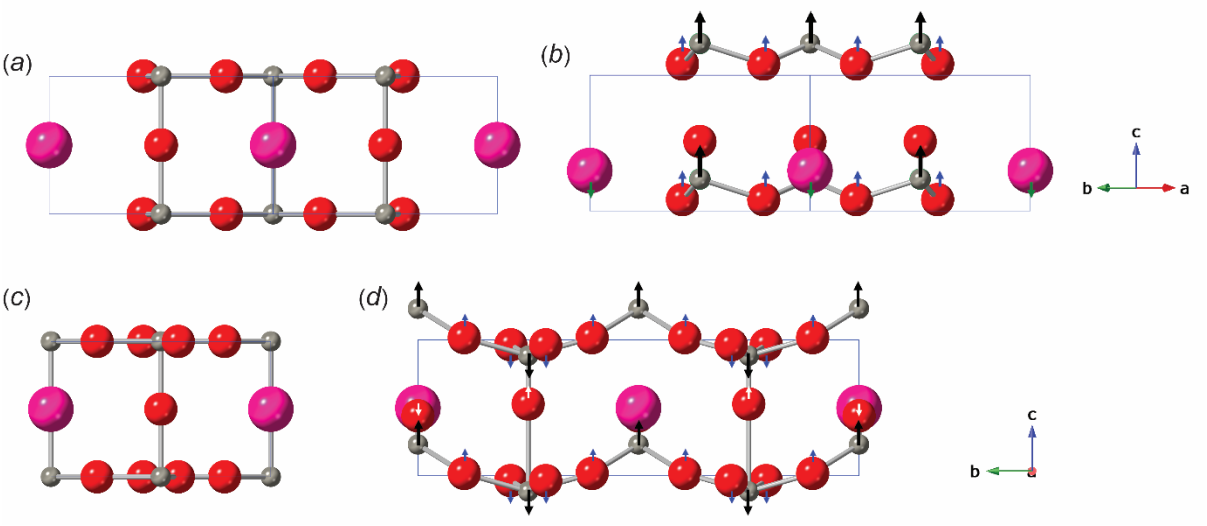

Figure S5 Aristotype *P*6/*mmm* unit cell (featuring no atomic displacements) viewed in the (a) (110) direction and (c) down the *a*-axis. Direction and relative size of atomic displacements of $RbNbW_2O_9$ for the polar displacive modes (b) Γ_2^- and (d) Γ_5^-. The arrows in the figure indicate the direction of the atomic displacement and the length of the arrows is chosen to be proportional to the magnitude of the atomic displacements at 288 K. Note the increased unit cell size when the Γ_5^- mode is active corresponding to an orthorhombic distortion.